

Geophysical Research Letters

RESEARCH LETTER

10.1029/2020GL091394

Key Points:

- Profiling floats equipped with oxygen sensors observed 30 cases of spring phytoplankton bloom in and around the Sea of Okhotsk, seasonal ice zone
- Total net community production estimated in the euphotic layer in cases where sea ice existed is much higher than that of no ice cases
- In addition to the intensification of surface stratification, sediment/iron released from melting sea ice likely enhances the spring bloom

Supporting Information:

- Supporting Information S1

Correspondence to:

S. Kishi,
sachiko-k@ees.hokudai.ac.jp

Citation:

Kishi, S., Ohshima, K. I., Nishioka, J., Isshiki, N., Nihashi, S., & Riser, S. C. (2021). The prominent spring bloom and its relation to sea-ice melt in the Sea of Okhotsk, revealed by profiling floats. *Geophysical Research Letters*, 48, e2020GL091394. <https://doi.org/10.1029/2020GL091394>

Received 28 OCT 2020

Accepted 3 MAR 2021

© 2021. The Authors.

This is an open access article under the terms of the [Creative Commons Attribution-NonCommercial License](https://creativecommons.org/licenses/by/4.0/), which permits use, distribution and reproduction in any medium, provided the original work is properly cited and is not used for commercial purposes.

The Prominent Spring Bloom and Its Relation to Sea-Ice Melt in the Sea of Okhotsk, Revealed by Profiling Floats

S. Kishi¹ , K. I. Ohshima^{2,3} , J. Nishioka^{2,3} , N. Isshiki^{1,4}, S. Nihashi⁵, and S. C. Riser⁶ 

¹Graduate School of Environmental Science, Hokkaido University, Sapporo, Japan, ²Institute of Low Temperature Science, Hokkaido University, Sapporo, Japan, ³Arctic Research Center, Hokkaido University, Sapporo, Japan, ⁴Hiroo Town Hall, Hiroo, Japan, ⁵Department of Engineering for Innovation, National Institute of Technology, Tomakomai College, Tomakomai, Japan, ⁶School of Oceanography, University of Washington, Seattle, WA, USA

Abstract Seven profiling floats equipped with oxygen sensors deployed in the Sea of Okhotsk provide time series data for 33 cases of spring phytoplankton bloom period, including 9 cases in which sea ice existed just before the bloom (prior-ice case). As an index of biological productivity, we calculated net community production (NCP) based on the increasing oxygen rate using the Redfield ratio. The total NCP in the euphotic layer averaged for prior-ice cases is $31.3 \text{ mmolC m}^{-2} \text{ day}^{-1}$, ~ 3 times higher than that of non-ice cases. In addition to intensification of surface stratification, other factors of sea-ice melt likely enhance the bloom. The influence of sea-ice melt is particularly large in the southwestern region, where the iron availability likely limits phytoplankton growth. A suggested scenario is that when the sea ice containing sediment/iron is transported from the northern shelves, a prominent bloom is induced via the iron supply by sea-ice melt.

Plain Language Summary The seasonal ice zone is a high biological productivity area with a large spring phytoplankton bloom. The enhanced biological production results in significant CO_2 uptake, which could play an important role in carbon budget. However, understanding of high biological productivity in seasonal ice zones is poor due to limited observations. This study examines the spring bloom in and around the Sea of Okhotsk, a typical seasonal ice zone, using profiling floats equipped with oxygen sensors. Based on the rate of oxygen increase for 30 cases of the spring bloom period, we estimated NCP as a quantitative indicator of biological production and CO_2 uptake. It is statistically shown that a large spring bloom, corresponding to high NCP, is strongly related to sea-ice melt. The cause is suggested to be sediments/iron released from melting sea ice as well as enhancement of stratification and light availability. This study will also provide the first attempt to evaluate the impact of significant sea ice decline in the Sea of Okhotsk on the carbon budget in the present and future.

1. Introduction

The seasonal ice zone generally provides a rich marine ecosystem, mainly originating from large phytoplankton blooms associated with sea-ice melt. The Sea of Okhotsk, a marginal sea of the North Pacific, is a typical such ocean (Mustapha et al., 2009; Sorokin & Sorokin, 1999). For example, Kasai et al. (2010) reported that the chlorophyll a concentration at a depth of 0–30 m in this sea increases just after sea-ice melt and peaks in April as $1.8 \pm 1.3 \text{ mg m}^{-3}$, which is much higher than that in the adjacent North Pacific (Shiozaki et al., 2014). Seasonal sea ice likely plays an important role in the enhancement of this spring phytoplankton bloom (hereafter referred to as the spring bloom). Specifically, the increased vertical stability of the fresh-water supply associated with sea-ice melt enhances light availability. This provides a favorable condition for the increase in phytoplankton (Niebauer et al., 1990; Sorokin & Sorokin, 1999), in addition to the enhanced nutrient supply provided by convective mixing in the preceding winter.

Most of the subarctic Pacific is regarded as the high nutrient low chlorophyll region, where the growth of phytoplankton is limited by iron (Tsuda et al., 2003). However, the Oyashio region of the western subarctic Pacific has relatively high biological productivity, likely due to the iron supply from the Sea of Okhotsk via intermediate water (Nishioka et al., 2007, 2013, 2020). The main iron sources in the Sea of Okhotsk are considered to originate from the Amur River (its mouth is located north of Sakhalin Island) and sediment on the continental shelf. The iron is incorporated into dense shelf water formed by sea-ice production, transported

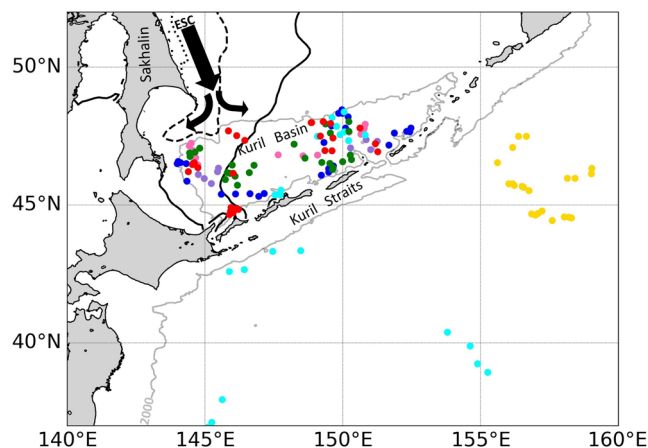


Figure 1. Locations of seven profiling float in April or May (spring bloom period) from 2007 to 2019. Each float is discriminated by color (further information on the floats is shown in Table S1). The black contours in the Sea of Okhotsk show the sea-ice edge (defined as 15% ice concentration) averaged over 2007–2018 for March (solid), April (dashed), and May (dotted). The 2,000 m isobaths are drawn by gray contours. The arrows represent the East Sakhalin Current.

by the East Sakhalin Current (black arrows in Figure 1), spread via the Okhotsk Sea Intermediate Water, and finally mixed vertically toward the surface by the strong tidal mixing in and around the Kuril Straits (Nishioka et al., 2014). The iron is also transported with Amur-diluted surface water, but its extent is confined to the northern shelf off Sakhalin Island due to scavenging by biological particulates. Other regions in the Sea of Okhotsk are considered to be iron-limited areas for phytoplankton growth, as other nutrients are likely in excess (see Figure S1 for the previous observations of nutrients and iron; Nishioka et al., 2014; Suzuki et al., 2014; Yoshimura et al., 2010).

On the other hand, sea ice in the southern region of the Sea of Okhotsk contains a higher concentration of iron than the underlying surface seawater, and the iron released by sea-ice melt provides a favorable condition for phytoplankton growth (Kanna et al., 2014, 2018). The enrichment of iron cannot be explained only by the atmospheric dust iron deposition onto the sea ice (Kanna et al., 2014). A part of sea ice in this region is transported from the shelf of Sakhalin Island and northwestern shelves of the Sea by the East Sakhalin Current and prevailing north wind (Simizu et al., 2014). Over these shelves, sedimentary materials, including iron, can be brought to the surface by the strong bottom currents and wintertime convection, and then incorporated into sea ice (Ito et al., 2017). Thus, there is a possibility that the iron in sea ice originates from the sedimentary materials over these shelves. However, all previous studies have

been based on a snapshot observation or single-point moored measurement. Owing to logistical difficulties of measuring in sea ice in these areas, no continuous observations during the spring bloom have been made. Thus, our knowledge of the spring bloom in the Sea of Okhotsk is very limited.

A quantitative indicator of marine biological production associated with the spring bloom is the net community production (NCP), which is equal to primary production minus respiration over all trophic levels. Estimations of NCP have been conventionally made by shipboard observations and/or moorings. However, these methods have a limitation in spatial coverage or monitoring period, and in general, observations that focus on NCP have not been conducted in ice-covered regions. Riser and Johnson (2008) was the first study that estimated an NCP from profiling floats equipped with oxygen sensors. They estimated the NCP just below the mixed layer in the Pacific subtropical ocean, based on the time series data of the oxygen vertical profile, using the Redfield ratio. This work has been followed by additional studies, which estimated the seasonal or annual NCP in various regions (e.g., Bushinsky & Emerson, 2015; Sukigara et al., 2011; Yang et al., 2017). Some of these studies have validated the use of oxygen variation for estimation of NCP by comparing it with estimates obtained from conventional methods. In recent years, Biogeochemical-Argo (BGC-Argo) floats, which can observe biogeochemical parameters such as oxygen, nitrate, pH, and chlorophyll *a*, have been deployed globally (Claustre et al., 2020). Many BGC-Argo floats have been deployed in the Southern Ocean through the Southern Ocean Carbon and Climate Observations and Modeling project (Johnson et al., 2017; Riser et al., 2018). These floats have observed a large spring bloom associated with sea-ice melt in the Southern Ocean (Briggs et al., 2018).

In the Sea of Okhotsk, 30 profiling floats have been deployed since 1997 (Ohshima et al., 2014), and those which were deployed after 2007 were equipped with oxygen sensors and a sea ice detection system. These floats can observe the time series of vertical profiles of water properties that cannot be captured by snapshot or satellite observations in this data-void region. Furthermore, owing to the sea ice detection system, the floats have provided year-round data, including the ice-covered season. Thus, it is expected that the data set might reveal the detail of bloom development process inferred from the change in water properties and its relationship with sea-ice melt process.

In this study, we analyze the behavior of dissolved oxygen (DO) in the upper ocean during the spring bloom, based on time series data of the vertical profiles obtained from the profiling floats with oxygen sensors. The study focuses on the effect and mechanism of sea-ice melt on the spring bloom by estimating the NCP

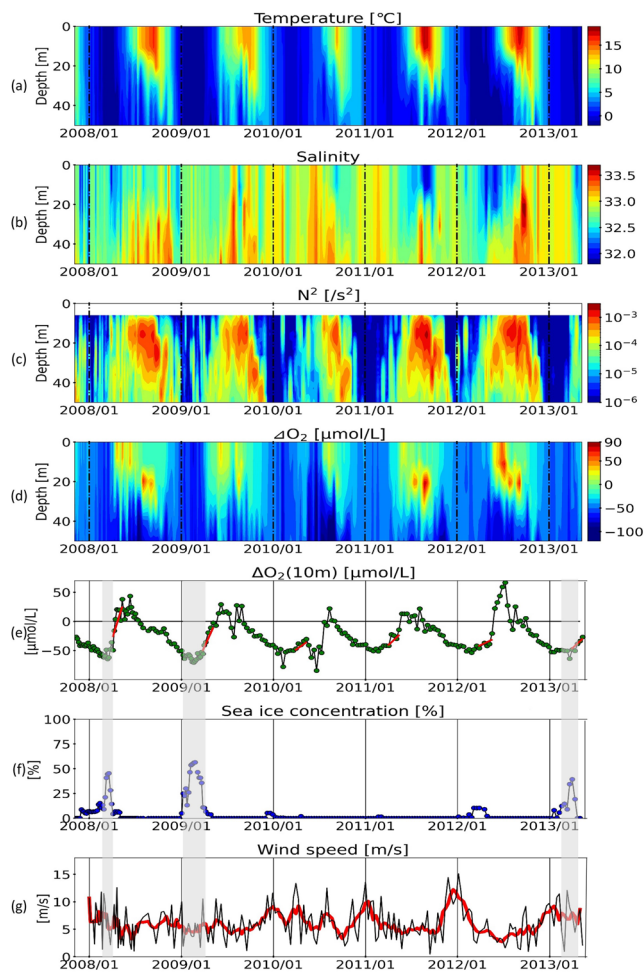


Figure 2. Time series of vertical profiles of (a) temperature, (b) salinity, (c) buoyancy frequency squared, represented as N^2 (d) ΔO_2 and (e) ΔO_2 at 10 m for float 5259 (red in Figure 1), and (f) sea-ice concentration from AMSR-E/2 and SSMIS and (g) wind speed from ECMWF, from October 2007 to May 2013. The red lines in (e) indicate least-squares fits, showing the increased rate of ΔO_2 during the spring bloom. The gray shades in (e–g) highlight the periods of sea-ice melt.

and comparing it with environmental conditions. The seven floats used in this study sampled a total of 33 cases of spring oxygen behavior over the course of 12 years, including 9 cases in which sea ice was present just before the spring bloom.

2. Data and Methods

2.1. Profiling Float Measurements

Seven profiling floats equipped with oxygen Optode sensors were deployed in the Sea of Okhotsk. The floats were ballasted to drift at a nominal depth of 1,650 m and programmed to cycle on a 5- or 10-day schedule. Although the Optode oxygen sensors have some bias errors, approximately 0 to $-40 \mu\text{mol kg}^{-1}$ for raw data and $-3.1 \pm 4.09 \mu\text{mol kg}^{-1}$ for calibrated data using the phase-domain method (Drucker & Riser, 2016), the sensor drift is negligible (Bushinsky et al., 2016) or only about 0.5% per year after deployment (preliminary analysis by Riser’s laboratory). In this study, we used the variation of raw oxygen data during a relatively short period to estimate the NCP of spring bloom. Thus, the use of uncalibrated oxygen data is unlikely to affect the conclusions of this study, even though the absolute value could be somewhat biased.

Each float was equipped with a sea ice detection system aimed at protecting the sensors from colliding with ice at the surface, as discussed in detail in Riser et al. (2018). When the float measures a temperature below a threshold value of -1.70°C in the near-surface mixed layer, close to the sea ice formation temperature, it immediately descends to the parking depth. The float would continue to cycle without surfacing until the measurements exceed the threshold temperature. Since the float does not surface during the under-ice period, its position during these periods is unknown and is estimated by linear interpolation between its last and first known locations. The trajectories of the seven floats used in this study are shown in Figure 1. The observation period ranges from November 2007 to December 2019 and covers 33 cases for the spring period.

2.2. Sea Ice and Wind Data

The presence of sea ice was determined by the daily ice concentration estimate from the Advanced Microwave Scanning Radiometers (AMSR-E/2) and the Special Sensor Microwave Imager/Sounder (SSMIS) as well as

by the temperature threshold of the floats. The ice concentration was estimated by using the Bootstrap algorithm (Comiso, 1995). The presence of sea ice before the onset of spring is ascertained by the following criteria: first, if the ice concentration averaged within a radius 100 km around a float’s surfacing position was above 30%; second, the sea ice concentration was above 20%, with the float’s ice detection system being activated. If either of these two conditions were met, we defined the case as having sea ice present (the gray shaded regions in Figure 2). Among the 33 cases in spring, 9 cases had sea ice just before the spring bloom.

The surface DO concentration is affected by various biological and physical factors. Air-sea gas exchange is the main physical factor and is a function of wind speed and temperature. To infer the magnitude of air-sea gas exchanges, we used daily wind speed at a 10-m height from the European Centre for Medium-Range Weather Forecasts Re-Analysis (ERA5) dataset, at grid points located closest to the surfacing locations of the floats.

2.3. Calculation of NCP

Because oxygen concentration also depends on seawater temperature and salinity, its variation is not necessarily simple. In this study, we used the oxygen anomaly ΔO_2 (oxygen concentration minus oxygen solubility), corresponding to negative AOU (Apparent Oxygen Utilization), to minimize the dependency on temperature and salinity. We followed the method by Riser and Johnson (2008) and calculated the NCP by using the rate of oxygen increase in spring. The period of the spring bloom is defined as the end of March through mid-May (40–50 days), and the rate of oxygen production is determined from the slope of straight lines fitted by least squares to the ΔO_2 data during each spring season. NCP rates are then estimated from these slopes at depths in the euphotic layer by converting oxygen production to carbon uptake using the Redfield ratio (150 moles of O_2 produced per 106 moles of C fixed (Anderson, 1995). We judged that the Redfield ratio is approximately valid for the spring bloom condition, with large diatoms predominating. The large diatom species are similar to those that appear in the western subarctic Pacific (Suzuki et al., 2014; Yan et al., 2020).

3. Results and Discussion

3.1. Time Series of Float Data

Time series of temperature, salinity, buoyancy frequency, and ΔO_2 from one of the profiling floats are shown in Figure 2, together with the sea-ice concentration and wind speed at the float locations. The float data clearly capture the seasonal cycle of the upper ocean. It is found that ΔO_2 at a depth of 10 m (Figure 2e) increased during spring (from the end of March to mid-May) each year. The change in ΔO_2 due to its dependence on salinity is only ~1%–3% of the total change. The increasing rate of ΔO_2 , estimated via least-squares fitting (the red line in Figure 2e), seems to depend on the observation year or position. The increasing rate is significantly higher in cases when sea ice cover existed just before the estimate (referred to as the prior-ice case), specifically in 2008 and 2009, than in cases with no prior sea ice cover (referred to as nonice case), specifically in 2010, 2011, and 2012. Such characteristics are commonly observed by the other six floats (see Figures S2–S7). In addition to the spring bloom, ΔO_2 showed a delayed peak at the surface from June to July in 2012, and a subsurface peak (20–30 m) from July to August in 2008, 2011, and 2012. This subsurface peak is consistent with the enhanced biological production characterized as a subsurface chlorophyll-a maximum in summer, as reported by Kasai et al. (2010). The analysis in this study focuses only on the spring bloom, which occurs from the end of March to mid-May, for examining the relationship between sea-ice melt and the spring bloom. Three of the non-ice cases did not show ΔO_2 increase in spring, and they are regarded as non-blooming (shown as gray crosses in Figure 4d). All other cases are regarded as blooming cases and used for NCP calculations.

Wind speeds in the observational area were generally higher in winter and lower in spring (Figure 2g). Variations of surface ΔO_2 (Figure 2d) do not show those expected from the wind variation, for example, oxygen supersaturation over 100%–110% occurred in April and May, even though the wind speed weakened in these months. As this tendency also occurred for the other floats (see Supplementary Figures S2–S7), the data suggest that these periods of supersaturation are not governed by air-sea gas exchanges that are controlled by wind speed. Furthermore, although the near-surface stratification in each spring was relatively strong, the increase in ΔO_2 at depth to 50 m occurred simultaneously. These suggest that this increment was caused mainly by in situ photosynthesis-related processes rather than by the atmospheric O_2 uptake.

After sea-ice melt, a salinity deficit occurs at the ocean surface. Examples of vertical profiles of salinity and temperature just after the ice melt and that of oxygen increment during the spring bloom are shown in Figure 3a and 3b, and one example for a non-ice case is shown in Figure 3c. The salinity and oxygen increment profiles correspond well with each other for prior-ice cases but not for non-ice cases (see supplementary for all the prior-ice cases [Figure S8] and non-ice cases [Figure S9] in the Sea of Okhotsk). In some of the non-ice cases, a low salinity layer is formed on the surface (Figure S9). However, the layer's temperatures were significantly higher than in the prior-ice cases, with no activation of the ice detection system. Thus, these low salinity layers were likely caused by the advection of low salinity water affected by the Amur River or East Sakhalin Current water. The salinity profile in these cases did not show good correspondence with the oxygen increment.

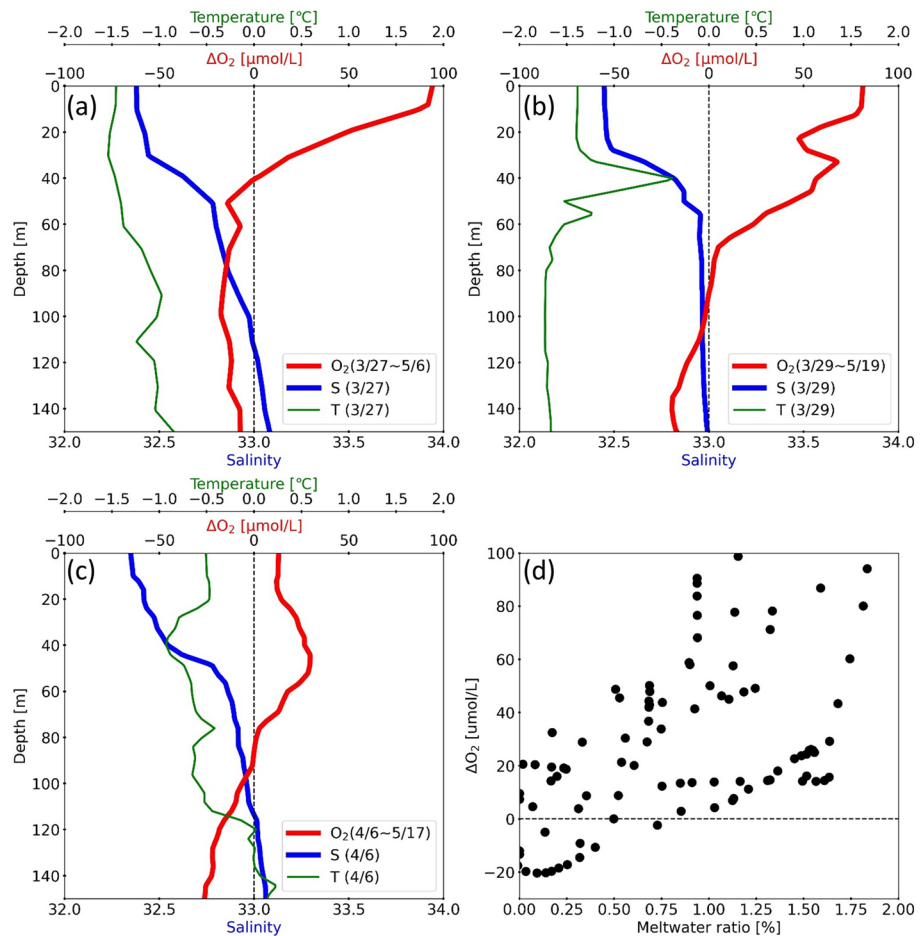


Figure 3. Vertical profiles of salinity (blue lines) and temperature (green lines) just after sea-ice melt and of DO increment during the spring bloom (red lines) for (a) the 2008 bloom (44.8°N, 146.0°E) and (b) the 2018 bloom (46.5°N, 144.1°E). (c) Same as (a) and (b) but for a non-ice case in 2011 (45.3°N, 146.8°E). (d) Plots of meltwater ratio versus oxygen increment during the spring bloom, estimated from all the prior-ice cases at 5 m intervals. DO, dissolved oxygen.

From the decrease of salinity, the content ratio of meltwater can be estimated based on the mixing ratio of salinity in sea ice (4.6 psu in the Sea of Okhotsk) and salinity in the source water (at the depth just below the base of the low-salinity layer). We have estimated the meltwater ratio from all the prior-ice cases at 5 m intervals, and examined its relationship with the oxygen increment (Figure 3d). A relatively strong correlation between the two (Correlation coefficient, R is 0.65) supports the idea that the oxygen increment due to photosynthesis is induced by the meltwater input, and further suggests that the strength of the spring bloom is governed by the amount of meltwater.

3.2. Estimation of NCP

The averaged vertical profiles of NCP derived from the float observations during the spring bloom are shown in Figure 4a, for prior-ice cases (9 cases) and non-ice cases (13 cases) in the Sea of Okhotsk, and for cases in which the floats were located in the North Pacific (8 cases). The NCP is by far highest in prior-ice cases, and the difference is more prominent near the surface. The total NCP for each individual spring bloom was calculated by vertical integration of the NCP profile data from 50 m to the surface, assumed to be the euphotic layer (Figure 4b). Calculations from greater depths show similar results: Calculations from 70 m result in the NCP increase only by less than 10% on average. The total NCP averaged for prior-ice cases is $31.3 \text{ mmolC m}^{-2} \text{ day}^{-1}$, which is ~ 2.7 times higher than the $11.6 \text{ mmolC m}^{-2} \text{ day}^{-1}$ of non-ice cases (99%

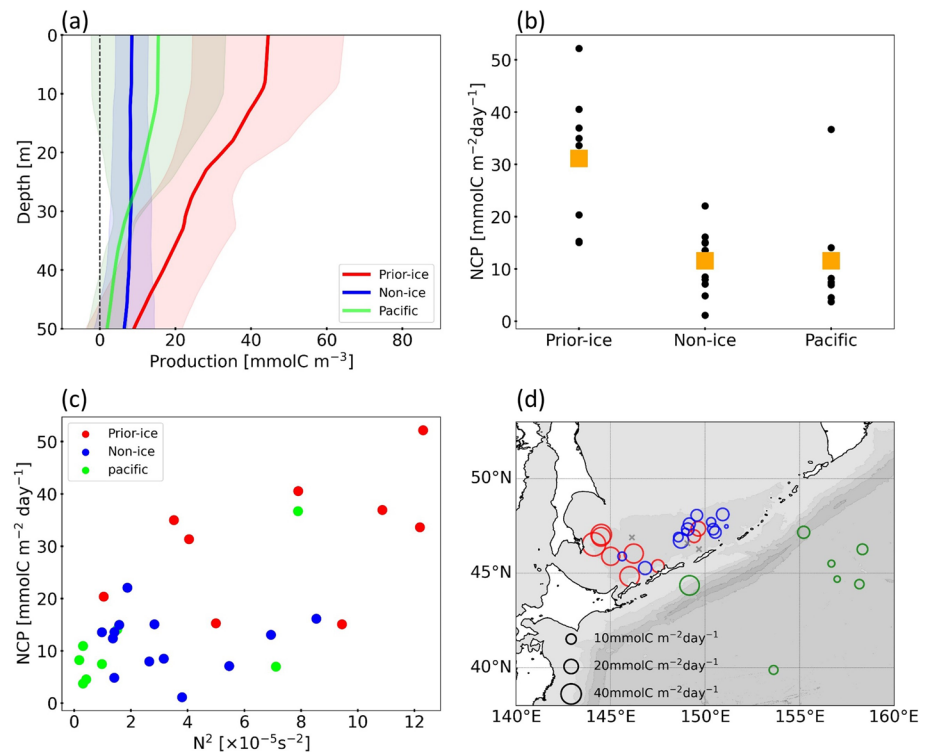


Figure 4. (a) Vertical profiles of NCP averaged for (red) prior-ice cases and (blue) non-ice cases in the Sea of Okhotsk and (green) cases in the North Pacific, with the standard deviations (indicated by shadings). (b) Total NCP integrated over the blooming layer for individual spring bloom (black dots) and the average (orange dots) classified into prior-ice cases and non-ice cases in the Sea of Okhotsk and cases in the North Pacific. (c) Plots of buoyancy frequency squared at a depth of 30 m versus total NCP. (d) Spatial distributions of total NCP during the spring bloom, with the circle size being proportional to the NCP value. The color coding in (c) and (d) follows that of (a). The contours in (d) indicate 50 m depth, obtained by the General Bathymetric Chart of the Oceans.

significance by the Student's *t*-test). This value is comparable to that in the Southern Ocean, known as the high biological production area (Thomalla et al., 2015). On average, the total biological production during the spring bloom period is 1,370 mmolC m⁻² for prior-ice cases and 500 mmolC m⁻² for non-ice cases. Note that air-sea gas exchanges are not considered in these NCP estimates. Since gas exchange would occur from sea to air when DO in the sea is supersaturated, the NCP found in this study probably tends to be an underestimate. However, as described in Section 3.1, it is likely that the oxygen increment in spring is mainly due to photosynthesis by biological production, and a qualitative discussion of the relationship between NCP and sea-ice melt is still adequate.

3.3. Effects of Sea-ice Melt

A spring bloom is a rapid biological increment occurring in mid-to-high latitudes due to the increase in sea temperature and solar illumination, which improve the environment for biological production. The current work is the first observation-based study that reveals the onset of a spring bloom induced by sea-ice melt in the Sea of Okhotsk, by showing significantly higher NCP in the prior-ice cases than in the non-ice cases. The analysis will now focus on how sea-ice melt affects the occurrence of spring bloom. This issue has not previously been well-understood, although the intensification of stratification at the surface layer from warming and the freshwater supply has been regarded as an important factor (Sullivan et al., 1993). Here, we compare the NCP values with the buoyancy frequency squared (N^2) averaged over 25–35 m depths (Figure 4c). During the spring bloom, the contribution of salinity to the density gradient (N^2) in the upper layer is 5–10 times larger than that of temperature. When sea ice was present just before, the near-surface stratification is increased mostly by freshwater input by ice melting. On average, N^2 is 7.4×10^{-5} ($/s^2$) for prior-ice cases, higher than the value of 3.2×10^{-5} ($/s^2$) for non-ice cases. Correlation between the stratification and

NCP ($R = 0.64$) suggests that the stratification is a factor for the spring bloom. While, for similar N^2 levels, the NCP tends to be higher in prior-ice cases than in non-ice cases (Figure 4c). These results suggest that the change in stratification is not the only reason why sea-ice melt leads to a massive spring bloom.

The locations of each spring bloom are plotted as circles in Figure 4d, with their size being proportional to the NCP values. Among the nine blooms in the western part of the Kuril Basin, defined as west of 147°E , the NCP value is significantly larger in the prior-ice cases (red) than in the non-ice cases (blue), by a factor of ~ 3 on average. In contrast, among 15 blooms in the eastern part of the Kuril Basin, defined as east of 147°E , there is no significant difference in the NCP value in cases between the prior-ice and non-ice cases. In the Sea of Okhotsk, the sea ice formed in the Sakhalin and northwestern shelves may incorporate bottom sediments containing iron, via strong winter convection reaching the bottom (Ito et al., 2017); after formation, the ice drifts to the southwestern region of the Sea of Okhotsk. We assume that a part of sea ice found in the southwestern part of the sea originates from these shelves, whereas sea ice in the eastern sea is locally formed in the Kuril Basin. We propose that the difference in the origin of sea ice explains the varying influence of sea-ice melt on the NCP.

It is also noted that, when the comparison is made for all the non-ice cases in the Sea of Okhotsk, the NCP tends to be larger in the area closer to the Kuril Straits. This may result from the advection of water including high nutrients and iron via the strong tidal mixing around the Kuril Straits (Nishioka et al., 2013).

4. Concluding Remarks

Seven profiling floats equipped with oxygen sensors had provided time series data for 33 cases of spring blooms, including 9 cases in which sea ice existed just before the spring bloom began (the prior-ice case), in and around the Sea of Okhotsk. Accumulation of these data makes it possible to statistically evaluate the effects of sea-ice melt on the spring bloom. All cases except three non-ice cases show that the oxygen in the surface layer increased during the spring, defined as the end of March to mid-May. As an index of biological productivity during the spring bloom, we estimated NCP based on the rate of oxygen increase and the Redfield ratio for these 30 cases. Among the blooming cases, the average total NCP in the euphotic layer of $31.3 \text{ mmolC m}^{-2} \text{ day}^{-1}$ in the prior-ice case is ~ 3 times higher than that in the non-ice case. These examples demonstrate that the sea-ice melt is a key factor for the prominent spring bloom.

We have examined how sea-ice melt affects the spring bloom. We used the buoyancy frequency squared averaged over depths of 25–35 m (typical euphotic zone depths) as an index of the stratification intensity during the spring bloom, and investigated its relationship with the total NCP. The NCP is always higher in the prior-ice cases than in the non-ice cases for similar buoyancy frequencies (Figure 4c). This suggests that other factors by sea-ice melt substantially enhance the spring bloom, in addition to the intensification of surface stratification.

In the Southern Ocean, a large spring bloom is likely to occur in many sea-ice melt regions (e.g., Briggs et al., 2018). In the case of the Sea of Okhotsk, the influence of sea-ice melt on the spring bloom seems to depend on the region. The influence of sea-ice melt is clearly identified in the southwestern region of the Sea of Okhotsk, while such influence is not so clear in the eastern region of the Kuril Basin. In the southwestern region of the Kuril Basin, where iron availability likely limits phytoplankton growth, only when the sea ice containing the sediment/iron is transported from the northern shelves, a prominent spring bloom is likely induced via the ice-supplied iron. If true, this scenario leads to further future studies seeking to make direct measurements of iron source and supply. By contrast, in the eastern Okhotsk region, water advected from the Kuril Straits may have supplied some iron from the lower layer via strong tidal mixing (Nishioka et al., 2013).

In this study, we estimated the NCP during the spring bloom in and around the Sea of Okhotsk, using the oxygen variability observed by a suite of profiling floats. Although our estimate is useful for evaluating the effect of sea-ice melt, the NCP estimates have some errors, mainly because the component of air-sea gas (oxygen) exchange cannot be incorporated. More accurate estimation would require time series data of nutrients such as nitrate and/or chlorophyll-a. The deployment of BGC profiling floats, which would make such observation possible, will be needed in the future. One ultimate goal, initiated from this study, is to examine

the CO₂ budget associated with the biological productivity in the Sea of Okhotsk and to determine the net exchange of CO₂ between the sea and the atmosphere throughout the annual cycle. For such a purpose, the annual NCP must be estimated with the evaluation of biological productivity in other seasons, such as during the subsurface summer phytoplankton bloom in addition to the spring bloom.

Data Availability Statement

The AMSR-E and SSMIS data were obtained from the website of the National Snow and Ice Data Center, University of Colorado (https://nsidc.org/data/ae_si12/versions/3; <https://nsidc.org/data/nsidc-0079/versions/3>). The AMSR2 data were provided by the Japan Aerospace Exploration Agency website (<https://gportal.jaxa.jp/gpr/?lang=en>). The ERA5 reanalysis data were obtained from the ECMWF Research Data Server (<https://cds.climate.copernicus.eu/cdsapp#!/dataset/reanalysis-era5-single-levels?tab=overview>). The data set of profiling floats can be seen from the website (<http://runt.ocean.washington.edu/hu/>).

Acknowledgments

The authors thank the anonymous reviewers for their insightful comments that have improved this study. Deployments of profiling floats were made under the cooperative study by Hokkaido University and the University of Washington. The profiling floats were prepared at the University of Washington by Dana Swift, Rick Rupan, and Dale Ripley through NOAA Grant NA15OAR4320063 to the Joint Institute for the Study of the Atmosphere and Ocean. The authors also thank Naoya Kanna, Masato Ito, Vigan Mensah, and Naoto Ebuchi for discussion and support on this study. This study was supported by Grants-in-Aid for Scientific Research (Grant nos. 17H00775, 17H01157, and 20H05707) from the Ministry of Education, Culture, Sports, Science and Technology in Japan.

References

Anderson, L. A. (1995). On the hydrogen and oxygen content of marine phytoplankton. *Deep Sea Research Part I: Oceanographic Research Papers*, 42, 1675–1680. [https://doi.org/10.1016/0967-0637\(95\)00072-E](https://doi.org/10.1016/0967-0637(95)00072-E)

Briggs, E. M., Martz, T. R., Talley, L. D., Mazloff, M. R., & Johnson, K. S. (2018). Physical and biological drivers of biogeochemical tracers within the seasonal sea ice zone of the Southern Ocean from profiling floats. *Journal of Geophysical Research: Oceans*, 123(2), 746–758. <https://doi.org/10.1002/2017JC012846>

Bushinsky, S. M., & Emerson, S. (2015). Marine biological production from in situ oxygen measurements on a profiling float in the subarctic Pacific Ocean. *Global Biogeochemical Cycles*, 29, 2050–2060. <https://doi.org/10.1002/2015GB005251>

Bushinsky, S. M., Emerson, S. R., Riser, S. C., & Swift, D. D. (2016). Accurate oxygen measurements on modified Argo floats using in situ air calibrations. *Limnology and Oceanography: Methods*, 14, 491–505. <http://dx.doi.org/10.1002/lom3.10107>

Claustre, H., Johnson, K. S., & Takeshita, Y. (2020). Observing the global ocean with Biogeochemical-Argo. *The Annual Review of Marine Science*, 12, 23–48. <https://doi.org/10.1146/annurev-marine-010419-010956>

Comiso, J. C. (1995). *SSM/I sea ice concentrations using the Bootstrap algorithm*. National Aeronautics and Space Administration Reference Publication.

Drucker, R., & Riser, S. C. (2016). In situ phase-domain calibration of oxygen Optodes on profiling floats. *Methods in Oceanography*, 17, 296–318. <https://doi.org/10.1016/j.mio.2016.09.007>

Ito, M., Ohshima, K. I., Fukamachi, Y., Mizuta, G., Kusumoto, Y., & Nishioka, J. (2017). Observations of frazil ice formation and upward sediment transport in the Sea of Okhotsk: A possible mechanism of iron supply to sea ice. *Journal of Geophysical Research: Oceans*, 122, 788–802. <https://doi.org/10.1002/2016JC012198>

Johnson, K. S., Plant, J. N., Coletti, L. J., Jannasch, H. W., Sakamoto, C. M., Riser, S. C., et al. (2017). Biogeochemical sensor performance in the SOCCOM profiling float array. *Journal of Geophysical Research: Oceans*, 122, 6416–6436. <https://doi.org/10.1002/2017JC012838>

Kanna, N., Sibano, Y., Toyota, T., & Nishioka, J. (2018). Winter iron supply processes fueling spring phytoplankton growth in a sub-polar marginal sea, the Sea of Okhotsk: Importance of sea ice and the East Sakhalin Current. *Marine Chemistry*, 206, 109–120. <https://doi.org/10.1016/j.marchem.2018.08.006>

Kanna, N., Toyota, T., & Nishioka, J. (2014). Iron and macro-nutrient concentrations in sea ice and their impact on the nutritional status of surface waters in the southern Okhotsk Sea. *Progress in Oceanography*, 126, 44–57. <https://doi.org/10.1016/j.pocean.2014.04.012>

Kasai, H., Nakano, Y., Ono, T., & Tsuda, A. (2010). Seasonal change of oceanographic conditions and chlorophyll a vertical distribution in the southwestern Okhotsk sea during the non-iced season. *Journal of Oceanography*, 66, 13–26. <https://doi.org/10.1007/s10872-010-0002-3>

Mustapha, M. A., Sei-Ichi, S., & Lihan, T. (2009). Satellite-measured seasonal variations in primary production in the scallop-farming region of the Okhotsk Sea. *ICES Journal of Marine Science*, 66(7), 1557–1569. <https://doi.org/10.1093/icesjms/fsp142>

Niebauer, H. J., Alexander, V., & Henrichs, S. (1990). Physical and biological oceanographic interaction in the spring bloom at the Bering Sea marginal ice edge zone. *Journal of Geophysical Research*, 95, C12. <https://doi.org/10.1029/JC095iC12p22229>

Nishioka, J., Nakatsuka, T., Ono, K., Volkov, Y. N., Scherbinin, A., & Shiraiwa, T. (2014). Quantitative evaluation of iron transport processes in the Sea of Okhotsk. *Progress in Oceanography*, 126, 180–193. <https://doi.org/10.1016/j.pocean.2014.04.011>

Nishioka, J., Nakatsuka, T., Watanabe, Y. W., Yasuda, I., Kuma, K., Ogawa, H., et al. (2013). Intensive mixing along an island chain controls oceanic biogeochemical cycles. *Global Biogeochemical Cycles*, 27, 920–929. <https://doi.org/10.1002/gbc.20088>

Nishioka, J., Obata, H., Ogawa, H., Ono, K., Yamashita, Y., Lee, K., et al. (2020). Subpolar marginal seas fuel the North Pacific through the intermediate water at the termination of the global ocean circulation. *Proceedings of the National Academy of Sciences of the United States of America*, 117(23), 12665–12673. <https://doi.org/10.1073/pnas.2000658117>

Nishioka, J., Ono, T., Saito, H., Nakatsuka, T., Takeda, S., Yoshimura, T., et al. (2007). Iron supply to the western subarctic Pacific: Importance of iron export from the Sea of Okhotsk. *Journal of Geophysical Research*, 112, C10. <https://doi.org/10.1029/2006JC004055>

Ohshima, K. I., Nakanowatari, T., Riser, S., Volkov, Y., & Wakatsuchi, M. (2014). Freshening and dense shelf water reduction in the Okhotsk Sea linked with sea ice decline. *Progress in Oceanography*, 126, 71–79. <https://doi.org/10.1016/j.pocean.2014.04.020>

Riser, S. C., & Johnson, K. S. (2008). Net production of oxygen in the subtropical ocean. *Nature*, 451, 327–325. <https://doi.org/10.1038/nature06441>

Riser, S. C., Swift, D., & Drucker, R. (2018). Profiling floats in SOCCOM: Technical capabilities for studying the Southern Ocean. *Journal of Geophysical Research: Oceans*, 123, 4055–4073. <https://doi.org/10.1002/2017JC013419>

Shiozaki, T., Ito, S. I., Takahashi, K., Saito, H., Nagata, T., & Furuya, K. (2014). Regional variability of factors controlling the onset timing and magnitude of spring algal blooms in the northwestern North Pacific. *Journal of Geophysical Research: Oceans*, 119, 253–265. <https://doi.org/10.1002/2013JC009187>

- Simizu, D., Ohshima, K. I., Ono, J., Fukamachi, Y., & Mizuta, G. (2014). What drives the southward drift of sea ice in the Sea of Okhotsk?. *Progress in Oceanography*, *126*, 33–43. <https://doi.org/10.1016/j.pocean.2014.05.013>
- Sorokin, Y., & Sorokin, P. Y. (1999). Production in the Sea of Okhotsk. *Journal of Plankton Research*, *21*(2), 201–230. <https://doi.org/10.1093/plankt/21.2.201>
- Sukigara, C., Suga, T., Saino, T., Toyama, K., Yanagimoto, D., Hanawa, K., & Shikama, N. (2011). Biogeochemical evidence of large diapycnal diffusivity associated with the subtropical mode water of the North Pacific. *Journal of Oceanography*, *67*, 77–85. <https://doi.org/10.1007/s10872-011-0008-5>
- Sullivan, C. W., Arrigo, K. R., McClain, C. R., Comiso, J. C., & Firestone, J. (1993). Distributions of phytoplankton blooms in the Southern Ocean. *Science*, *262*, 1832–1837. <https://doi.org/10.1126/science.262.5141.1832>
- Suzuki, K., Hattori-Saito, A., Sekiguchi, Y., Nishioka, J., Shigemitsu, M., Isada, T., et al. (2014). Spatial variability in iron nutritional status of large diatoms in the Sea of Okhotsk with special reference to the Amur River discharge. *Biogeosciences*, *11*, 2503–2517. <https://doi.org/10.5194/bg-11-2503-2014>
- Thomalla, S. J., Racault, M.-F., Swart, S., & Monteiro, P. M. S. (2015). High-resolution view of the spring bloom initiation and net community production in the Subantarctic Southern Ocean using glider data. *ICES Journal of Marine Science*, *72*, 1999–2020. <https://doi.org/10.1093/icesjms/fsv105>
- Tsuda, A., Takeda, S., Saito, H., Nishioka, J., Nojiri, Y., Kudo, I., et al. (2003). A mesoscale iron enrichment in the western subarctic Pacific induces a large centric diatom bloom. *Science*, *300*, 958–961. <https://doi.org/10.1126/science.1082000>
- Yan, D., Yoshida, K., Nishioka, J., Ito, M., Toyota, T., & Suzuki, K. (2020). Response to sea ice melt indicates high seeding potential of the ice diatom *Thalassiosira* to spring phytoplankton blooms: A laboratory study on an ice algal community from the Sea of Okhotsk. *Frontiers in Marine Science*, *7*, 613. <https://doi.org/10.3389/fmars.2020.00613>
- Yang, B., Emerson, S. R., & Bushinsky, S. M. (2017). Annual net community production in the subtropical Pacific Ocean from in situ oxygen measurements on profiling floats. *Global Biogeochemical Cycles*, *31*, 728–744. <https://doi.org/10.1002/2016GB005545>
- Yoshimura, T., Nishioka, J., & Nakatsuka, T. (2010). Iron nutritional status of the phytoplankton assemblage in the Okhotsk Sea during summer. *Deep Sea Research Part I: Oceanographic Research Papers*, *57*, 1454–1464. <https://doi.org/10.1016/j.dsr.2010.08.003>